NUCLEATION LIMIT OF THE PLANAR LOOP HEAT PIPE

[1]Junwoo Suh, [2]Debra Cytrynowicz, [1]Frank M. Gerner, and [2]H. Thurman Henderson

[1] *Department of Mechanical, Industrial and Nuclear Engineering,*
[2] *Department of Electrical, and Computer Engineering and Computer Science,*
University of Cincinnati, Post Office Box 210072 Cincinnati, Ohio, 45221-0072,
(513) – 556 – 4774, suhj@email.uc.edu

ABSTRACT

The Loop Heat Pipe (LHP) under development is a next generation micro heat transfer device that utilizes the latent heat of a working fluid and has excellent transfer capacity compared with that of standard metallic cooling devices. A typical LHP consists of an evaporator, a reservoir (also called the compensation chamber), vapor and liquid lines, a subcooler, and a condenser. As heat is applied to the evaporator, input energy is used for the evaporation of liquid in the pores of the primary wick or leaks to the compensation chamber. The nucleate boiling, which occurs below the primary wick in the evaporator, is a very significant phenomena. It affects critical operating issues, such as dry out of the primary wick. Using a transparent evaporator with a highly polished inner surface, the nucleation, which occurred in the evaporator, was studies. The relation between the temperature and pressure of the working fluid in the chamber, nucleate boiling variables, was also studied. De-ionized water was utilized as the working fluid.

INTRODUCTION

The loop heat pipe (LHP) is a sort of thermal control and heat transport device developed in the former Soviet Union in the mid 1980's, and has been employed in a reliable and versatile thermal control system for the space applications. The LHP can transport very large thermal power loads over long distances through flexible, small diameter tubes and against high gravitational heads. LHPs are two-phase heat transfer devices that utilize the phenomena of evaporation and condensation to transfer heat and are completely self-circulating systems that have no mechanical moving parts and add no unwanted vibration to the spacecraft.

The Planar Loop Heat Pipe at University of Cincinnati

The traditional loop heat pipe that was proposed by Maidanik et al. [1] in 1985 has a cylindrical configuration and an amorphous porous wick. A family of planar loop heat pipes is being developed at the University of Cincinnati. The work being conducted is based upon the use of a radically different type of wick structure made of planar coherent porous silicon (CPS). Using this technology, it is possible to achieve arrays of densely stacked micrometer sized capillaries or pores, which are essentially identical in diameter, in the common semiconductor material, silicon. This is in contrast to conventional amorphous porous ceramic wicks, which have pores of various diameters. In these wicks the largest pore dictates the value of the burst-through pressure and compromises the upper power level achievable by the loop heat pipe. Coherent porous silicon technology avoids such compromises through its uniformity. The resulting configuration is planar, which is more convenient for surface cooling applications for electronics, such as space solar power cells, and other flat or gently curved surfaces [2].
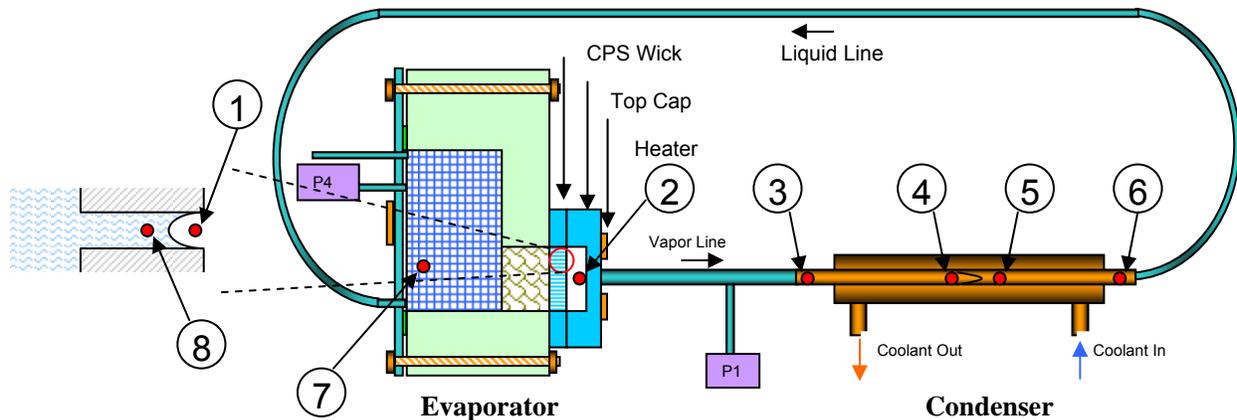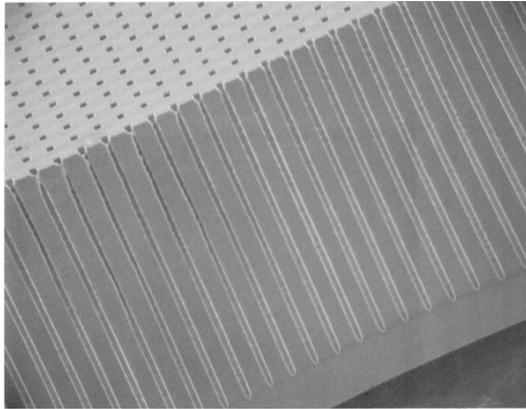

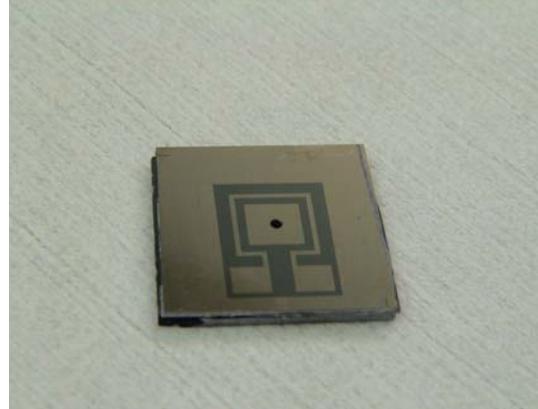**Figure 1: Schematic of the planar loop heat pipe**

A schematic of the planar loop heat pipe, which is being developed at the University of Cincinnati, is shown in Figure 1. The device consists of an evaporator, condenser, a liquid reservoir (also called the compensation chamber or hydro-accumulator), and separate liquid and vapor lines. The compensation chamber is thermally and hydro-dynamically connected to the evaporator. Inside the evaporator of the planar loop heat pipe, there is a coherent porous silicon wick structure, which maintains the separation between the liquid and vapor phases. In addition to the primary wick inside the evaporator, a secondary wick is situated between the compensation chamber and evaporator. It ensures that liquid remains available to the wick at all times.

The very novel CPS technology was utilized in the fabrication of the porous wick in the loop heat pipe. Figure 2 (a) is a SEM micrograph of a sample of coherent porous silicon before through-holes have been produced. During post processing, an aqueous solution of potassium hydroxide is used to etch the wafer backside of the sample to open the pores and produce the wick. The CPS wick consists of an array of coherent pores produced by the photo-electrochemical dissolution of silicon in an aqueous solution of hydrofluoric acid. Its pores have an approximate diameter of 5 micrometers and the pitch, or center-to-center spacing, is 20 micrometers. The porosity pictured is 6.25 percent [3, 4]. The CPS wick was made from a two-

inch n-type (100) silicon wafer and was bonded to the top layer (Figure 2 (b)). A nickel heater was integrated onto the backside of the silicon wafer to apply the uniform heat. The superheated vapor in the chamber of top cap exits through the hole to which the vapor line is soldered.

(a) Coherent porous silicon wick

(b) Top cap

Figure 2: CPS wick and top cap

Thermodynamics of the planar Loop Heat Pipe

The operating principle of the planar LHP is summarized as follows. As heat is applied to the evaporator, liquid is vaporized. Menisci, which are formed at the liquid-vapor interface in the evaporator wick, are supported by capillary forces even though pressure forces push them down. Vapor condenses in the condenser and the capillary forces continue to push liquid back to the evaporator. The applied heat from the heat source provides the driving force for the circulation of the working fluid and no external pumping power is required.
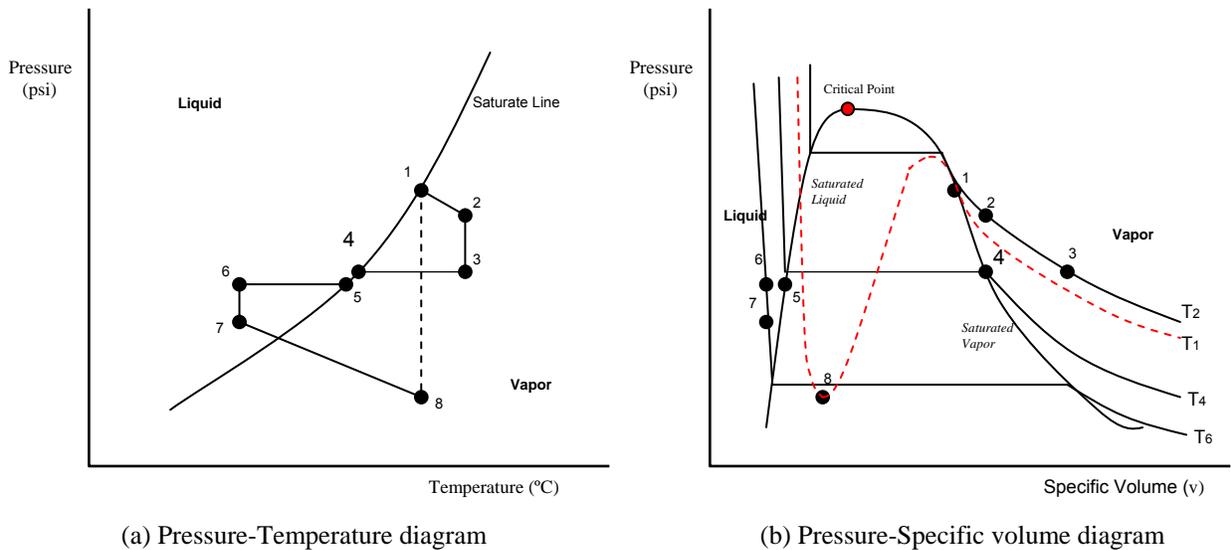

(a) Pressure-Temperature diagram

(b) Pressure-Specific volume diagram

Figure 3: The P-T and P-v diagram of the loop heat pipe (not to scale)

Figure 3 (a) and (b) show the thermodynamic states of the working fluid at each of the physical locations shown in Figure 1. At point 1, just above the liquid-vapor interface in the pores of primary wick, the fluid is vaporized at the saturation temperature T_1 and pressure P_1. As the vapor flows through the vapor accumulation area, it becomes superheated at the exit of the evaporator (point 2) due to heating and a pressure drop. Assuming the vapor transport line to be perfectly insulated, the temperature of the vapor will remain unchanged. Because the pressure continues to drop along the vapor line, the vapor becomes more and more superheated, relative to the local saturation pressure, until it reaches the entrance of the condenser (point 3). The vapor loses its sensible heat and begins to condense inside the condenser (point 4). Between points 4 and 5, the pressure drops through the condenser tube and the saturated vapor condenses to saturated liquid. At point 5 vapor condensation is completed. The liquid continues to be subcooled until it exits the condenser at point 6. Because the liquid transport line is well insulated, the process between points 6 and 7 is an adiabatic process with a pressure drop. The subcooled liquid enters the compensation chamber at point 7. The heat leak from the primary wick heats the subcooled liquid in the compensation chamber. At point 8, the temperature of liquid equals that of saturated vapor (point 1). Even though point 8 is indicated in the vapor region in Figure 3 (a) the liquid in the pores of the primary wick is superheated liquid. Due to the input power, this superheated liquid evaporates to saturate vapor in a constant temperature precesses with the pressure change across the meniscus [5, 6].
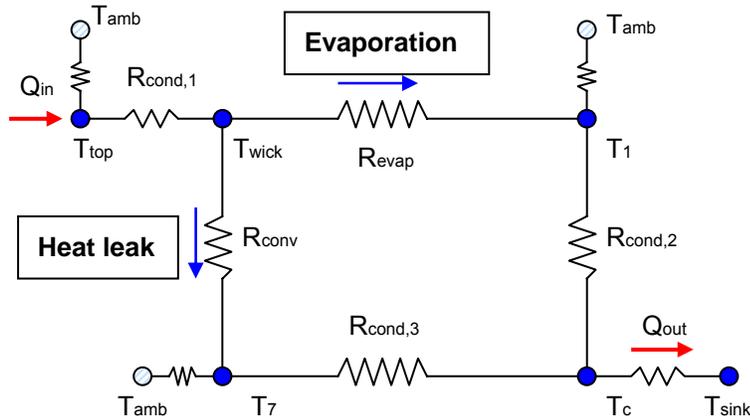

Figure 4: Thermal resistance network

Figure 4 shows the thermal resistance network of the planar loop heat pipe. The input power (Q_{in}) is conducted to the primary wick. By neglecting the heat loss to the ambient, all of the input energy goes into the evaporation of the liquid in the pores of the primary CPS wick or leak to the bottom.

$$\dot{Q}_{in} = \dot{Q}_{evapration} + \dot{Q}_{heat \cdot leak} = \dot{m}h_{fg} + hA(T_{wick} - T_7) \qquad (1)$$

It is necessary to monitor any nucleate boiling, which occurs inside the evaporator of the micro loop heat pipe. If nucleate boiling occurs on the bottom side of the coherent porous silicon wick, it could lead to wick "depriming" and cause equipment failure.

Nucleation Limit

There are several operating limits in the planar loop heat pipe; such as, the capillary, sonic, entrainment, superheated liquid and nucleate boiling limits. The nucleation limit, specifically, is considered here. Nucleate boiling, by definition, is characterized by the preferential formation of vapor bubbles at certain locations known as "nucleation sites". This occurs when the liquid temperature is increased to a temperature above the saturation temperature in contact with a surface [7]. The classical equation for the nucleate boiling is:

$$r_c = \frac{2\sigma T_{Sat}}{\rho_v h_{fg}\left(T_{Wall} - T_{Sat}\right)} \tag{2}$$

The minimum cavity mouth radius for nucleation to occur at a nucleation site is given by r_c. The onset of nucleate boiling can be predicted if the relation between the surface roughness, the pressure of the evaporator chamber, and the temperature of the surface is established.

Hamdan et al. [8] proposed the steady state LHP model which was described by conservation equations, thermodynamic relations, capillary and nucleate boiling limits. The seven major independent equations consisted of seven unknown independent variables, T_1, T_8, T_7, $\dot{m}$, β, $\rho_{v,h}$, $\rho_{v,cc}$, and were solved using a simple iteration technique which took into account the proper boundary conditions. The maximum superheated temperature (ΔT_t) in the liquid was:

$$\Delta T_t = \left(\frac{v_{fg,c}T_c}{h_{fg,c}}\right)\left[\frac{8\mu_{l,c}\dot{m}(l-l_v)}{\pi\rho_{l,c}R^4} + \frac{8\mu_{v,c}\dot{m}l_v}{\pi\left(\frac{\rho_{v,c}+\rho_{l,c}}{2}\right)R^4} + \frac{8\mu_{l,c}\dot{m}L}{A\varepsilon\rho_{l,c}r^2}\right] \tag{3}$$

and should be less than the nucleate boiling limit (ΔT_{max}) for the proper operation of the whole system.

$$\Delta T_t \le \Delta T_{max} \approx \frac{2\sigma T_{sat}}{\rho_v h_{fg}R_a} \tag{4}$$

A nucleate boiling limit was also suggested by Hamdan et al [9]. The nucleate boiling limit (ΔT_{max}) was calculated by measuring the actual R_a (average RMS roughness) value of the liquid side of the CPS wick even though Hamdan et al. used the pore radius. This limit was compared with the maximum superheated temperature (ΔT_t) solved by the mathematical model. In this way, the maximum heat load could be predicted.
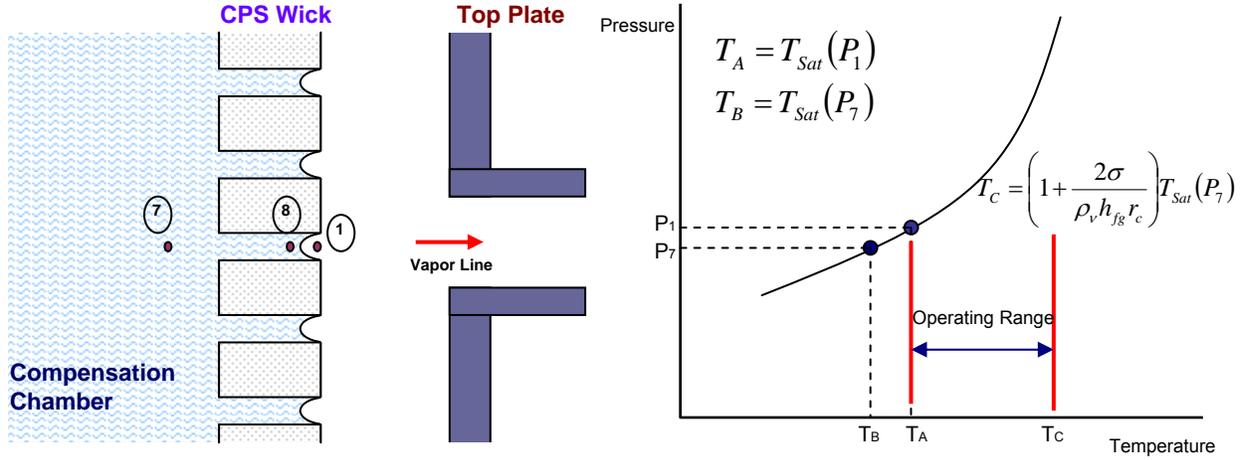
(a) Steady state condition in the evaporator   (b) Pressure-temperature curve

Figure 5: System operation region

When the heat is applied through the top cap, the temperature difference between the upper and bottom side of CPS wick is not much due to the high thermal conductivity of the silicon. The pressure in the upper chamber (P_1) is higher than the pressure in the compensation chamber (P_7). T_A is the saturation temperature corresponding to the upper chamber (P_1).

$$T_A = T_{Sat}(P_1) \tag{5}$$

The temperature, T_B, is the corresponding value of pressure in compensation chamber (P_7) on the saturation curve.

$$T_B = T_{Sat}(P_7) \tag{6}$$

The wall temperature (T_{wall}) can be acquired from the Equation (2).

$$T_C = T_{wall} = \left(1 + \frac{2\sigma}{\rho_v h_{fg} r_c}\right) T_{Sat}(P_7) \tag{7}$$

Like Figure 5 (b), the system operating range can be predicted. When the primary wall temperature (T_{wall}) is less than T_A there is no evaporation in the pores of CPS wick. Because the temperature does not reach the saturation temperature the liquid remains in the subcooled condition. If the wall temperature is passed through the temperature, T_C, then it is easier to initiate the nucleate boiling from the bottom side. Once the nucleate boiling is occurred bellowed the primary wick it is undesirable for the proper operation in two aspects. First, majority of input energy go for the heat leak to the compensation chamber. This can be shut down the pumping mode which pushes the liquid in the evaporator to the condenser. Second, the vapor layer, which would form below the CPS wick, would also block fluid flow through the loop.

EXPERIMENTAL SETUP AND PROCEDURE

To understand the nucleation, which occurred below the primary wick in the evaporator, two different series of tests were conducted. One was a basic study to understand the relation between the pressure and temperature of liquid in the chamber. The second concerned the nucleation that occurred in the evaporator during operation. These tests were made possible through the use of a transparent evaporator.

See-Through Evaporator

The evaporator is an essential part of entire closed loop system. The phenomena occurring in it must be well understood for proper operation. To monitor and study nucleation in the evaporator, a clear evaporator, which consisted of a top plate and a compensation chamber, was constructed from Pyrex glass.
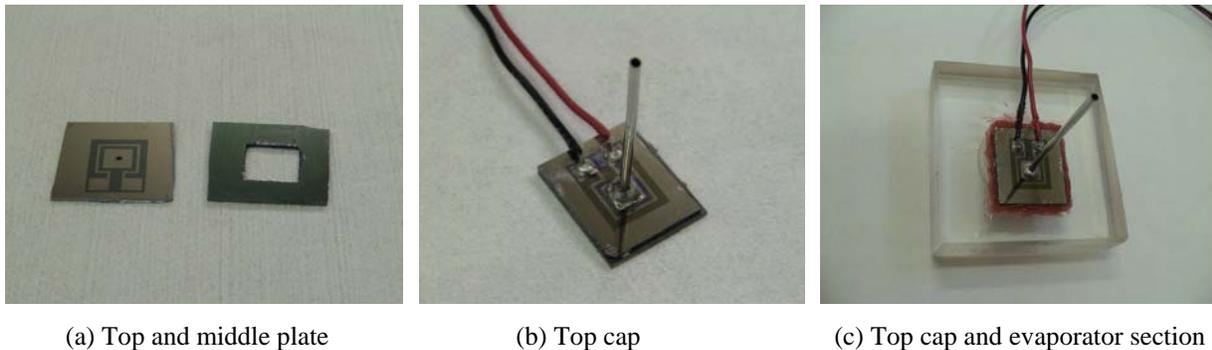

| (a) Top and middle plate | (b) Top cap | (c) Top cap and evaporator section |

FIGURE 6: Photographs of the top cap and compensation chamber.

The top cap consisted of three layers. The top layer was a nickel heater integrated onto one side of a silicon wafer to provide the uniform application of heat to the primary coherent porous silicon wick through the middle frame layer. The middle silicon layer was a one square centimeter area etched into a 1.7 by 1.7 square-centimeter piece of silicon. The etched area functioned as the vapor collection chamber (Figure 6 (a)). The bottom layer was a primary coherent porous silicon wick. To protect against leakage, these three plates were bonded together with VACSEAL and baked in an oven for one hour at 260 ºC. As is shown in Figure 6 (b), the top cap was connected by solder to a stainless steel tube to which the vapor transport line was attached. The stainless steel tube was four centimeters in length, and had an inner diameter of one millimeter and an outer diameter of 1.5 millimeters. The top cap was positioned in the evaporator section, which consisted of a Pyrex 7740 glass compensation chamber and a Pyrex glass back plate. The split-level compensation chamber consisted of two cylindrical volumes, each of which had its own diameter. A diamond drill was used to produce the two different sized volumes. The diameters and lengths of the smaller and larger volumes, respectively, were 1.0 centimeter and 0.6 centimeters and 2.54 centimeters and 0.9 centimeters. The glass back plate enabled visual observation of the activity below the CPS wick during the tests. High-Temp RTV SILICONE was chosen as the sealant to bond together the top cap and evaporator section because it made it possible to separate the top cap from the evaporator section without damage to the Pyrex glass surface.
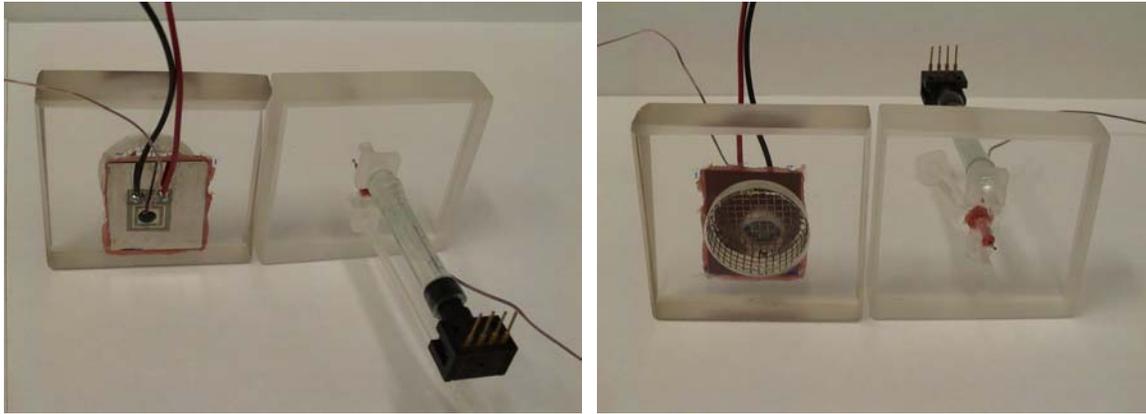
| (a) Outside surface of the evaporator | (b) Inside surface of the evaporator |

FIGURE 7: Top cap, evaporator section and back Pyrex glass plate.

The transparent Pyrex glass back plate was designed to seal the compensation chamber in the evaporator section and to enable observation of the phenomena, which occurred below the CPS wick. Three holes were machined into the back plate with a diamond drill. One hole was the input for the pressure sensor. A thermocouple to the compensation chamber was placed through the second hole, which was then sealed with silicone. The working fluid was supplied through the third hole, which was linked to the transparent liquid line after filling. Figure 7 shows the outside and inside sections of the transparent evaporator. The stainless steel retaining mesh was used in the compensation chamber only when the secondary wick, quartz wool, was utilized in the evaporator to secure it in place below the primary CPS wick (Figure 7 (b)). The evaporator section and back glass plate were also sealed with Silicone RTV.

Relation between the Pressure and Temperature

First, a basic study was conducted to understand the relation between the pressure and temperature of the working fluid in the chamber. The evaporator section and Pyrex glass back plate were used to observe nucleate boiling on the silicon surface. The silicon wafer had a nickel heater integrated onto the polished side. The opposite side of the heater plate was an unpolished surface with a roughness of approximately 0.2453 micrometers. The roughness of the unpolished surface of the silicon wafer was characterized in terms of the RMS roughness (R_a) using a KLA Tencor P-10 Profiler. A type-T thermocouple was epoxied to the top plate to measure its temperature. The temperature difference between the inner and outer surfaces of the chamber was less than 0.7 °C due to the high conductivity of silicon. It was verified through the pre-test that the plate was well insulated. De-ionized water was used as the working fluid. An OMEGA PX26 series pressure transducer was used to monitor the chamber pressure. As in Figure 8 (a), pressure was applied to the chamber by the hydraulic head (H). Heat was uniformly applied through the integrated heater on the silicon plate. The activity inside the device was observed through the glass back plate. A vapor bubble with a diameter larger than 200 micrometers was clearly seen by means of the zoom function of a SONY camcorder.
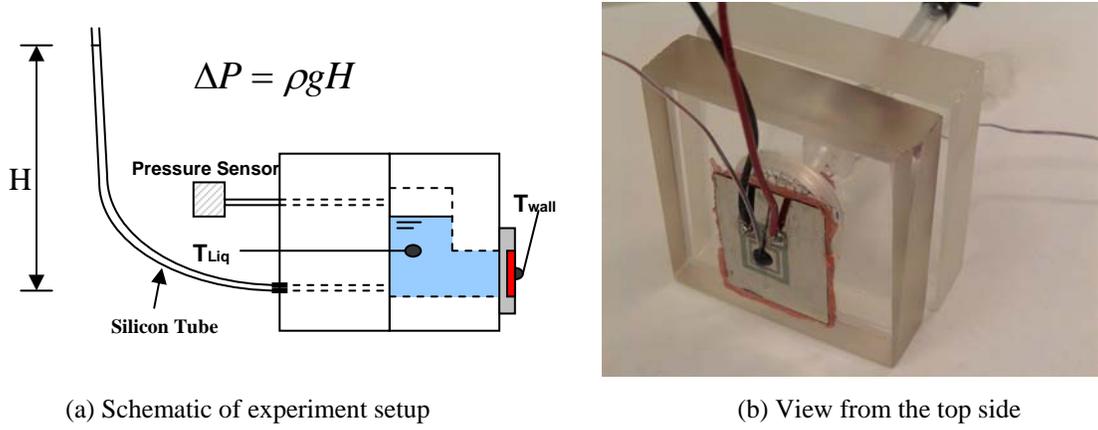
$$\Delta P = \rho g H$$

(a) Schematic of experiment setup

(b) View from the top side

Figure 8: A basic study about the nucleation

Vertical Orientation

Figure 9 shows a nucleation test conducted with the see-through evaporator. Type T thermocouples were used to measure the temperature of the top cap and liquid in the compensation chamber. A pressure sensor was connected to the compensation chamber to measure pressure at the bottom side of the primary CPS wick. The insulation was only placed on the top cap side to insulate against heat leakage to the ambient.

Before heat was applied to the evaporator, 3.5 milliliters of de-ionized water, the working fluid, were injected into the compensation chamber with a syringe. No de-gassing procedure was performed. The total volume of the compensation chamber was 4.6 milliliters. After the compensation chamber had been filled with the working fluid, the liquid transport line, a transparent silicone tube, was connected to the reservoir by a plastic connector (Figure. 9 (b)). Due to the capillary force of the primary CPS wick there was no liquid flow to the vapor line. The input power was calculated from the power supply voltage and current settings. A camcorder was used to film the activity observed at the bottom of the CPS wick. After the system reached a steady state condition, liquid which condensed from vapor in the vapor line was collected in a graduated cylinder.
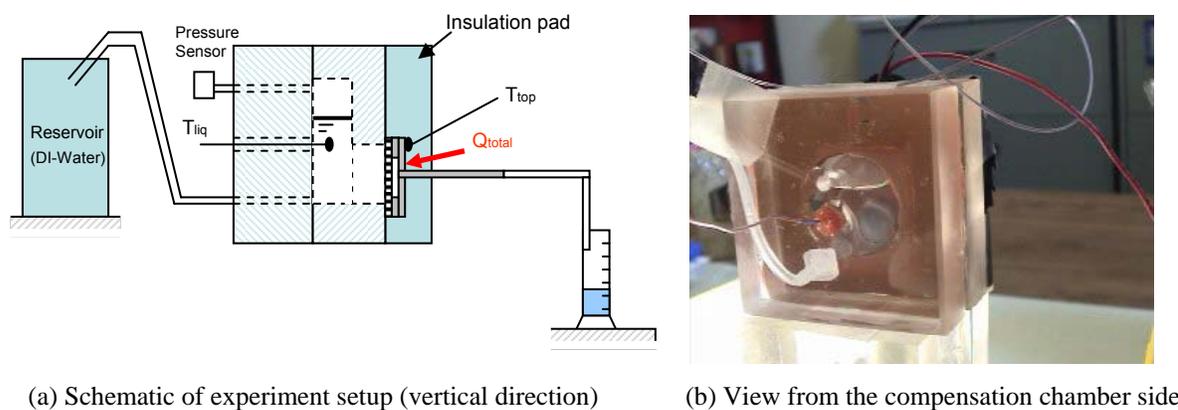

(a) Schematic of experiment setup (vertical direction)

(b) View from the compensation chamber side

Figure 9: Schematic and photograph of the experiment with the visualized evaporator

RESULTS AND DISCUSSION

Relation between the Pressure and Temperature

Using the silicon wafer, which had an RMS roughness value of 0.2453 micrometers, the nucleate boiling experiment was conducted to understand the relation between the pressure and temperature of liquid in the chamber. Figure 10 shows the surface temperature versus the pressure of the chamber. The state of the chamber was monitored and temperatures were recorded when the vapor bubbles formed on the surface and generated from the silicon surface at a rate of five per second or five Hertz (Table 1). With the zoom function of SONY camcorder, the vapor bubble with the 200-micrometer diameter was clearly monitored. The de-gassing process was not conducted because it was not easy to insert the working fluid into the evaporator without again dissolving air. The onset point of vapor bubbles was around 65 °C. This value was much less than the saturation temperature because de-ionized water was utilized as a working fluid without any de-gassing process. The vapor bubbles rose to the top from the surface when the temperature of the silicon was 101.3 °C at atmospheric pressure. The pressure in the chamber was changed with the different hydraulic head. The trend under nucleate boiling conditions in the chamber was similar to the saturation curve even though the temperatures were superheated several degrees.
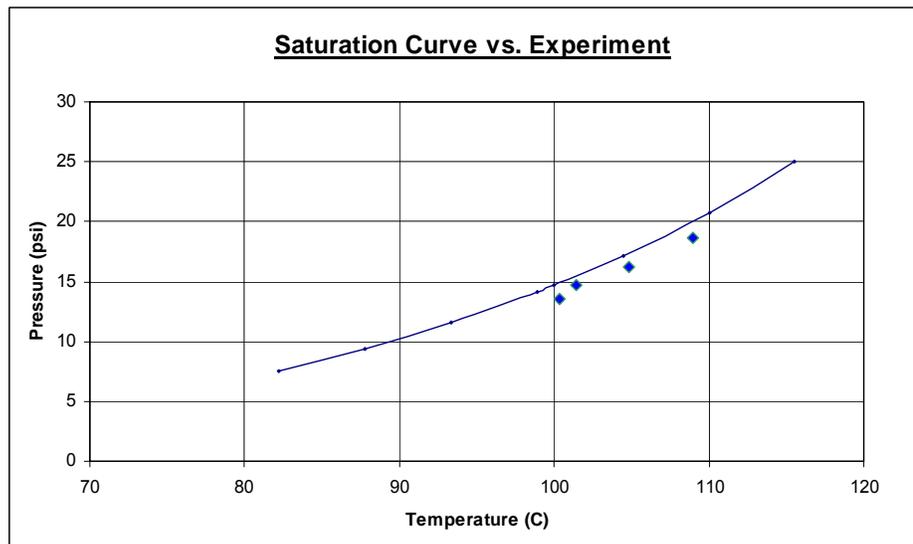

**Figure 10: Nucleate boiling curve (Temp. vs. Pressure)**

Table 1. Nucleate boiling pressure vs. Temperature

| Pressure (psi)	Wall Temp. (ºC)	Liquid Temp.(ºC)
13.6	100.3	75.7
14.7	101.4	74.7
16.2	104.8	77.8
18.7	109.0	82.2

"Pumping" Mode in the Evaporator

A primary CPS with a capillary pressure of 3.444 pounds per square inch was utilized without the secondary wick in the compensation chamber. The average pore radius was assumed to be 5.437 micrometers. The initial temperature of entire system was 23.5 ℃ and gradually increased as 9.39 Watts was applied to the top plate heater. Vapor bubbles formed on the CPS wick surface at quite a low temperature compared to the saturation temperature because it was not under vacuum and air was still dissolved in the de-ionized water (Figure 11 (a)). As the temperature of the CPS wick increased, the volumes of the vapor bubbles also increased. Shown in Figure 11 (b), the formed vapor bubbles rose and merged together at the top area on the wick due to buoyancy. The large bubble, which formed at the top area of the CPS wick, rose to the liquid-air interface and the tiny bubbles formed again. These vapor bubbles increased and decreased in volume as if they were breathing. Other groups have also observed this "breathing wick" phenomenon [10]. As liquid condensed in the vapor line, it fluctuated back and forth (Figure 11 (c)). It was assumed that the liquid evaporated in the pores of the primary CPS wick and then condensed in the stainless steel tube due to its low temperature. The system reached and remained in a steady state condition for one and half hours. The big vapor bubble remained at the top site continuously increased its volume and rose up. Many of the small vapor bubbles reformed on the surface of CPS wick. They were "breathing in and out" in synchronization with the fluctuating condensed liquid. The top plate temperature was 101.3 ℃ and the liquid temperature in the compensation chamber was 80.5 ℃. The amount of condensed liquid, which poured down from the vapor line into the graduated cylinder, was measured. Assuming that all of the collected liquid was due to evaporation, the amount of liquid collected in twenty-five minutes was 7.6 milliliters. The corresponding evaporation energy was calculated to be 11.436 Watts. From this result, it was speculated that there was some unknown mechanism, which pushed the liquid to the vapor line, because the output energy exceeded the input energy.

Several tests were conducted at various input powers. At the input powers of 6.86 Watts and 9.39 Watts, the activity below the CPS wick prior to reaching steady state was similar to the previous description. Some amount of liquid was collected from the vapor line even though the mechanism was not yet understood. No liquid was collected at low input powers such as 4.16 Watts. At the input power of 12.63 Watts there was a period during which liquid was collected. When the temperature of the top plate suddenly increased to approximately 134 ℃ the collection of liquid stopped. Unlike in the previous test, nucleate boiling was observed on the CPS wick and the liquid in the vapor tube stopped fluctuating (Figure 11 (d)). One possible explanation for this phenomenon is that all of the energy went into the nucleate boiling.
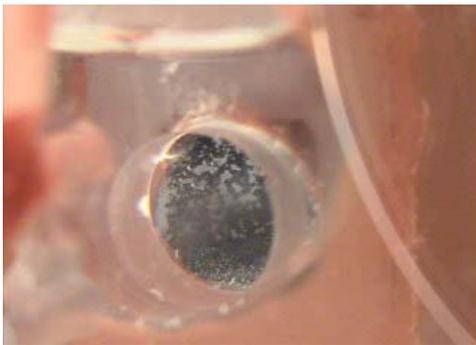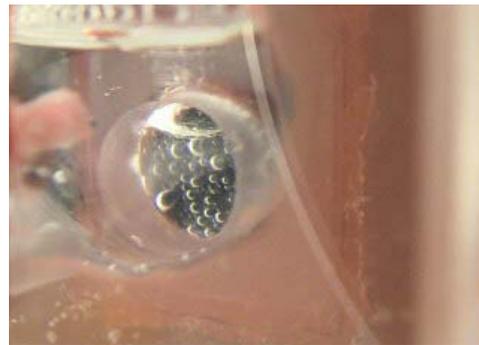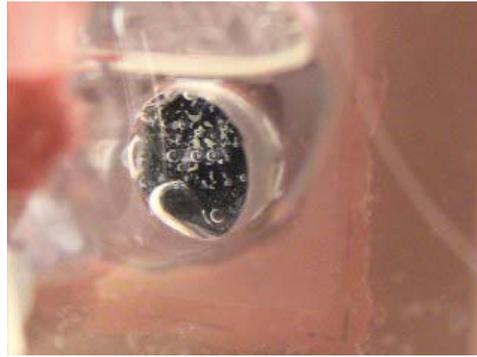

| (a) Vapor bubbles onset | (b) breathing vapor on the CPS wick |
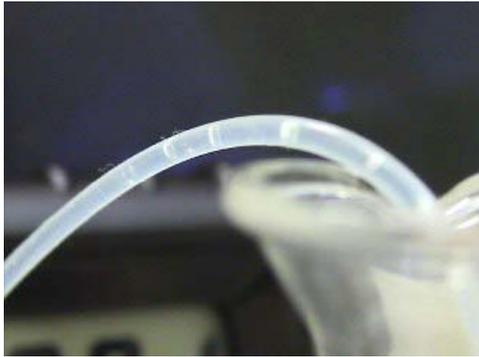
(c) Fluctuating liquid condensed in the tube   (d) Nucleate boiling below the CPS wick

FIGURE 11: "Pumping" Mode in the evaporator of planar loop heat pipe

Three Regions

Attempts to measure the temperature of the CPS wick were abandoned because the CPS wick is so easily damaged and pores in the wick were blocked if the thermocouple was attached to the surface with the epoxy. The temperature of top plate and the liquid in the evaporator were measured instead of the CPS wick. The measured value of the top plate temperature was suspicious; a little low due to the thick layer of epoxy between the surface and tip of thermocouple.
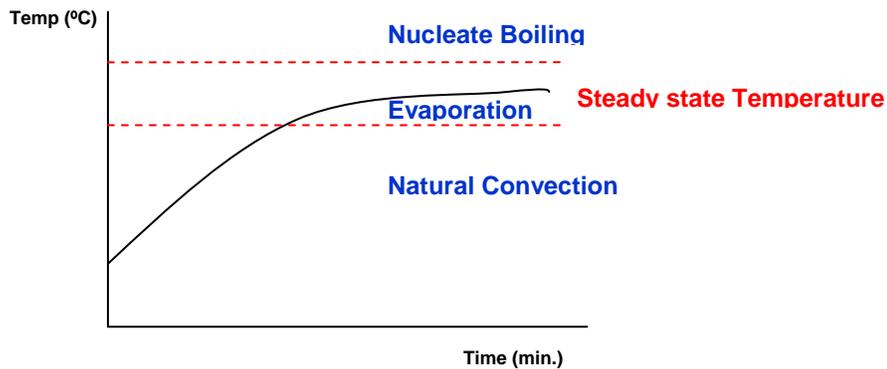

Figure 12: Nucleate boiling curve (Temp. vs. Pressure)

Table 2. Steady state temperature of top plate and liquid

Q	4.16 W	6.864 W	9.39 W	12.63 W
Ttop	92.3	94.3	101.3	133.9
Tliq	72.3	76.8	80.5	84.6
Pumping	×	O	O	O → ×

The time during which the CPS wick reached the steady state temperature depended on the input power. As shown in Figure 12, it was assumed that there were three regions: natural convection, evaporation, and nucleate boiling. If the steady state temperature was reached in the natural convection region, as in the test in which 4.16 Watts was applied, vapor bubbles formed only on the surface. If this temperature was reached in the evaporation region, the volumes of the vapor bubbles expanded and contracted. A "pumping" mode was observed. In the case of 12.63 Watts of input power, as the transient temperature of the wick passed the natural convection and evaporation regions, the vapor bubbles formed and their volumes oscillated. As the wick temperature passed the maximum temperature and reached the nucleate boiling region, nucleate boiling below the CPS wick was observed. Once the nucleate boiling occurred the liquid which had condensed in the tube stopped fluctuating. No liquid from the vapor line was collected. The majority of the input energy was wasted on nucleate boiling and not in evaporation.

Secondary Wick

The function of secondary wick was to keep the wick wet and collapse the vapor bubbles, which formed below the CPS wick. Quartz wool was used as a secondary wick to monitor its effect. The amount of 0.0087 grams was inserted into the smaller volume of the split-level compensation chamber. The stainless steel retaining mesh was used to push the secondary wick to the primary wick. Its porosity of the secondary wick was calculated to be 92 %. An input power of 7.13 Watts was applied to the evaporator. The steady state temperatures reached by the top plate and liquid were 114.7 °C and 62.6 °C, respectively. In this case, there was no liquid condensing from the vapor line even though there was pumping in the test at the same without the secondary wick. It was speculated that the vapor bubbles, which formed in the secondary wick due to their high radii, blocked the area below the primary wick. "Depriming" occurred and shut down the pumping operation in the evaporator.
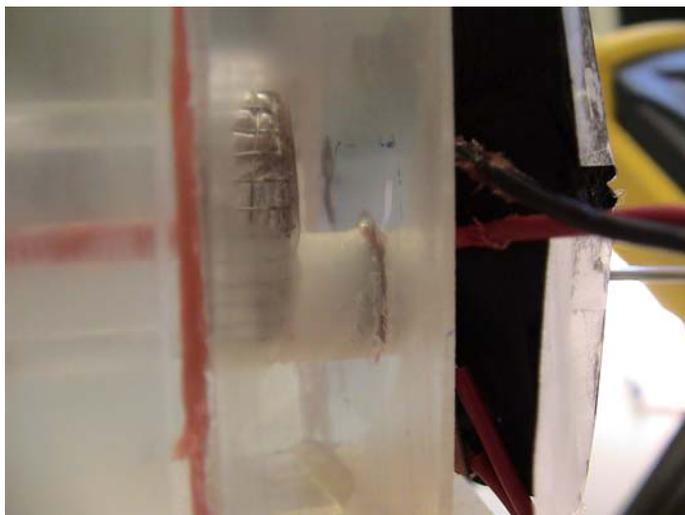

Figure 13: Secondary wick in the compensation chamber

CONCLUSIONS

The trend under nucleate boiling conditions in the chamber was similar to the saturation curve even though the temperatures were superheated several degrees. The vapor bubbles onset temperature in the surface was much less than the saturation temperature due to the dissolved gas.

There was an operating range in which the liquid could be properly pumped from the compensation chamber to the vapor line. That range is depending on the temperature of primary wick. The pumping mechanism was not observed at low input powers. In the case of the high input power, all of the energy caused nucleate boiling on the backside of the primary wick. Pumping ceased when nucleate boiling was observed in the evaporator. The nucleate boiling is significant factor in determining the nucleation limit and deprime.

In the vertical orientation, full deprime was not observed due to buoyancy and the pumping mode did not stop even though the primary wick was partially deprimed. It should be noted that orientation also affects the nucleation limit.

It was assumed that the secondary wick would collapse any vapor bubbles that formed below the primary wick. That was not true in this test with the 92 % porosity quartz wool. Vapor bubbles formed in the secondary wick due to large radii and caused deprime of the primary wick. The density of the secondary wick should be considered a very important variable.

ACKNOWLEDGEMENTS

REFERENCES

1. Maidanik, Y., Vershinin, S., Kholodov, V., and Dolggirev, J., 1985, "Heat Transfer Apparatus", US patent 4515209.
2. Cytrynowicz, D., Medis, P., Parimi, S., Shuja, A., Henderson, H.T., and Gerner, F.M., "The MEMS Loop Heat Pipe Based on Coherent Porous Silicon – The Modified System Test Structure," in *proceedings of Space Technology and Applications International Forum (STAIF-2004)*, edited by M. El-Genk, AIP Conference Proceedings 669, New York, 2004, pp. 164-173.
3. Cytrynowicz, D., Hamdan, M., Medis, P., Shuja, A., Henderson, H.T., Gerner, F.M., and Golliher, E., "MEMS Loop Heat Pipe Based on Coherent Porous Silicon Technology," in *proceedings of Space Technology and Applications International Forum (STAIF-2002),* edited by M. El-Genk, AIP Conference Proceedings 608, New York, 2002, pp. 220-232.
4. Hölke, A., Pilchowski, J., Henderson, H. T., Saleh, A., Kazmierczak, M., Gerner, F. M., Baker, K., "Coherent Macroporous Silicon as a Wick Structure in an Integrated Micro-

Fluidic Two - Phase Cooling System," *Proceedings of the SPIE Conference on Microfluidic Devices and Systems*, Santa Clara, California, September 21 - 22, 1998.

5. Ku, J., "Operating characteristics of loop heat pipes," Society of Automotive Engineers, 1999-01-2007, 1999.

6. Atabaki, N., and Baliga, B.R., "Steady-State Operation of a Loop Heat Pipe: Network Thermofluid Model and Results," *Proceeding of 2003 ASME International Mechanical Engineering Congress,* paper No. IMECE2003-43968, pp. 73-85, 2003.

7. Kandlikar, S.G., Shoji, M., and Dhir, V.K., "Nucleat Boiling", Handbook of Phase Change: Boiling and Condensation, Editor Kandlikar S., Shoji M., and Dhir V., 1999, Ch. 4, pp 71-120.

8. Hamdan, M., Cytrynowicz, D., Medis, P., Shuja, A., Gerner, F.M., and Henderson, H.T., 2002, "Loop Heat Pipe (LHP) Development by Utilizing Coherent Porous Silicone (CPS) Wicks," *ITHERM International Conference on Thermal Phenomena in Electronic Systems*, San Diego, California

9. Hamdan, M., Gerner, F.M., and Henderson, H.T., 2003 "Steady state model of a loop heat pipe (LHP) with coherent porous silicon (CPS) wick in the evaporator", *19th Annual IEEE Semiconductor Thermal Measurement and Management Symposium (SEMI-THERM)*.

10. Ku., J., Swanson, T.D., Herold, K., and Kolos, K., "Flow Visualization within a Capillary Evaporator," *SAE international,* Warrendale, PA, SAE paper No. 932236: pp. 1424-1432, 1993.

11. Cytrynowicz, D., Hamdan, M., Medis, P., Henderson, H.T., Gerner, F.M., and Golliher, E., "Test Cell for a Novel Planar MEMS Loop Heat Pipe Based on Coherent Porous Silicon," in *proceedings of Space Technology and Applications International Forum (STAIF-2003)*, edited by M. El-Genk, AIP Conference Proceedings 654, New York, 2003, pp. 227-238.

NOMENCLATURE, ACRONYMS, ABBREVIATIONS

A : Wick cross sectional area, m^2

CPS   : Coherent porous silicon

H   : Heat transfer coefficient, $J/m^2 \cdot K$

h_{fg} : Latent heat of evaporation, J/kg

l : Tube length, m

L : Wick thickness, m

$\dot{m}$: Mass flow rate, kg/s

R : Tube radius, m

R_f : Surface roughness, m

T_{Sat} : Saturation temperature, K

T_{Wall} : Surface temperature, K

Greek symbols

ε : Porosity

β : Volumetric ratio, $V_{v,cc} / V_{cc}$

μ : Dynamic viscosity, kg/s·m

ρ_v : Vapor density, kg/m^3

σ : Surface tension, N/m

Subscript

c   : Condenser

cc   : Compensation chamber

l   : Liquid

v   : Vapor